

# Statistical theory of phenotype abundance distributions: a test through exact enumeration of genotype spaces

JUAN ANTONIO GARCÍA-MARTÍN<sup>1,2,3</sup>, PABLO CATALÁN<sup>1,4</sup>, SUSANNA MANRUBIA<sup>1,2</sup> and JOSÉ A. CUESTA<sup>1,4,5,6</sup>

<sup>1</sup> *Grupo Interdisciplinar de Sistemas Complejos (GISC), Madrid, Spain*

<sup>2</sup> *Programa de Biología de Sistemas, Centro Nacional de Biotecnología (CSIC), Madrid, Spain*

<sup>3</sup> *Bioinformatics for Genomics and Proteomics, Centro Nacional de Biotecnología (CSIC), Madrid, Spain*

<sup>4</sup> *Departamento de Matemáticas, Universidad Carlos III de Madrid, Leganés, Madrid, Spain*

<sup>5</sup> *Instituto de Biocomputación y Física de Sistemas Complejos (BIFI), Universidad de Zaragoza, Spain*

<sup>6</sup> *UC3M-BS Institute of Financial Big Data (IFiBiD), Universidad Carlos III de Madrid, Getafe, Madrid, Spain*

PACS 87.10.-e – General theory and mathematical aspects  
 PACS 87.15.A- – Theory, modeling, and computer simulation  
 PACS 87.23.Kg – Dynamics of evolution

**Abstract** –The evolutionary dynamics of molecular populations are strongly dependent on the structure of genotype spaces. The map between genotype and phenotype determines how easily genotype spaces can be navigated and the accessibility of evolutionary innovations. In particular, the size of neutral networks corresponding to specific phenotypes and its statistical counterpart, the distribution of phenotype abundance, have been studied through multiple computationally tractable genotype-phenotype maps. In this work, we test a theory that predicts the abundance of a phenotype and the corresponding asymptotic distribution (given the compositional variability of its genotypes) through the exact enumeration of several GP maps. Our theory predicts with high accuracy phenotype abundance, and our results show that, in navigable genotype spaces—characterised by the presence of large neutral networks—, phenotype abundance converges to a log-normal distribution.

**Introduction.** – How the genetic information maps into functional phenotypes (the so-called genotype-to-phenotype, or GP, map) critically conditions the dynamics of evolution [1, 2]. Genotypes encode the information to generate phenotypes and in the process of replication undergo all sorts of mutations. The second basic mechanism of evolution, selection, acts upon phenotypes. Standard approaches to evolutionary dynamics have traditionally overlooked the fact that genotype and phenotype are connected through very complex mechanisms, and that the latter may have strong effects on the dynamics.

Genotype spaces can be depicted as networks, with nodes representing genotypes and links joining pairs of genotypes mutually accessible through a mutation. Phenotypes are then subsets of nodes in this network, and the GP map describes their distribution in genotype space. As selection acts on phenotypes, evolution within a connected component of a phenotype is neutral (or nearly so). For this reason, they are referred to in the literature as neutral networks (NNs) [3, 4]. A characteristic feature of all

known GP maps is the strongly heterogeneous distribution of the abundance (number of nodes) of their NNs [5, 6]. A few NNs are huge, typically percolating the whole genotype space, whereas most of them are small. This has evolutionary implications. First of all, the existence of huge NNs endows populations with a high genomic variability without bearing any selective cost. Secondly, most phenotypes are not accessible for entropic reasons [7–9]. Besides, large NNs are so interwoven that virtually any pair of them are connected to each other, thus facilitating the search for phenotypes [10, 11]. Under this paradigm, evolution is both robust and innovative.

Given the complexity of GP maps, we need to uncover and characterise as many general features as possible. One of them is the abundance distribution of NNs. The first studies of this distribution often relied on random samplings of the genotype space and considered relatively short RNA molecules [12, 13]. These are chains of a two- to four-letter alphabet (A, U, C, G or a subset of those), whose phenotype is identified as a minimum-free-

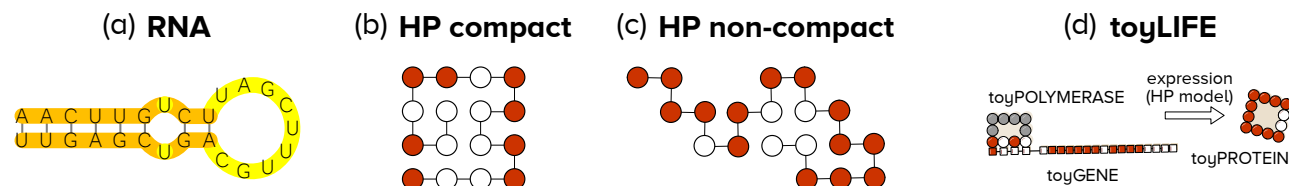


Fig. 1: Schematic representation of the different GP maps exhaustively studied in this work. (a) In RNA, sequences are folded to minimum free energy secondary structures that define the phenotype; (b) in the compact version of the HP model, hydrophobic (H, white circles) and polar (P, red circles) residues adopt the minimum compact energy configuration; (c) in non-compact HP, sequences are assigned to self-avoiding walks of minimum energy; (d)  $\text{toyLIFE}$  is a multilevel GP map with HP-like sequences that code for compact HP interacting proteins. Phenotype definitions can be found in Appendix A.

energy folding (secondary structure) [14]. Results pointed to a fat-tailed, decaying distribution [13,15–18]—although whether exponential, power-law, or otherwise is far from clear. Later studies of longer molecules (up to 126 letters long) show bell-shaped abundance distributions instead [8].

The first theoretical model addressing this question considered a set of binary sequences with a specific GP mapping rule [19]: the abundance distribution was an unequivocal power law. Later, it was pointed out that two different kinds of distributions—power-law and log-normal—are possible [20]. The argument relies on the existence of sites showing low and high compositional variability within a phenotype. Power laws are expected when these positions occupy fixed sites, whereas log-normals arise if their location is not fixed, so that counting the number of arrangements of them in the sequence yields a combinatorial factor. In the case of RNA sequences, low/high variability sites are associated to paired/unpaired nucleotides in the folded structure. A combinatorial calculation of the distribution of paired and unpaired sites can be carried out exactly (see [21] and references therein) and shown to be normal. As the number of low variability sites can be related to the logarithm of the phenotype abundance, the resulting distribution turns out to be log-normal. As a matter of fact, since not only paired sites, but any other structural feature of the folded chain can be shown to have a normal distribution, the argument can be extended even if site variability is affected by other structural elements. The log-normal prediction is thus expected to be quite robust.

**Versatility of a site.**— An alternative way to look at the problem of estimating phenotype abundance was suggested in the discussion of [20]. If, for a given phenotype, a variable  $v_i$  could measure the average number of different letters of the alphabet that show up at site  $i$  of its sequences, then the abundance could be estimated as

$$S_{\text{est}} = v_1 v_2 \cdots v_L \quad (1)$$

if the genotype is a chain of length  $L$ . This definition is easy to understand if sites are either completely neutral (any mutation maintains the phenotype,  $v_i = k$ , the size of the alphabet) or fully constrained (any mutation changes

phenotype,  $v_i = 1$ ). In a more general case,  $v_i$  would take intermediate values.

Given that phenotypes differ in the distributions of their structural motifs, and that the variability of a site is strongly correlated to the motif it sits in, variables  $v_i$  can be regarded as phenotype-dependent random variables that take values from a certain distribution. Thus, by the central limit theorem  $\ln S$  will be a phenotype-dependent, normally-distributed random variable.

Here is a way to estimate one such variable  $v_i$  (henceforth referred to as *versatility*) for an alphabet of  $k$  letters. We choose a phenotype and count in how many of its genotypes letter  $\alpha$  shows up at site  $i$ . Let  $m_{\alpha,i}$  be that number. Then we define the versatility at site  $i$  through

$$v_i = \frac{1}{M_i} \sum_{\alpha=1}^k m_{\alpha,i}, \quad M_i \equiv \max\{m_{1,i}, \dots, m_{k,i}\}. \quad (2)$$

The rationale behind this definition relies on assuming that the relative frequencies of each letter of the alphabet at each position  $i$  are proportional to the fraction of the space of genotypes associated to the phenotype. It implicitly assumes that the most frequent letter at each position is always characteristic of the phenotype, while other letters, appearing less frequently, may yield sequences corresponding to different phenotypes. For example, if G appears  $m_{G,i}$  times and C appears  $m_{G,i}/2$  times, other letters being absent, the versatility of that site would be  $v_i = 3/2$ , meaning that a half of the mutations from G to C at that site change phenotype. When only one letter appears,  $v_i = 1$ , while  $v_i = k$  if all letters are equally likely, recovering the limits of simple models [19,20].

**Testing the definition of versatility.**— In order to show that the versatility introduced in Eq. (2) is a meaningful concept, we have tested it for different GP maps (sketched in Fig. 1) regarding how well it predicts the abundance of a specific phenotype component and its relationship with the distribution of phenotype abundances.

First, we have folded all RNA sequences of length  $L = 16$ , using the Vienna package [22], and classified them according to their secondary structures. For such a small length, phenotypes are normally fragmented into several connected, neutral components (NCs) of comparable size,

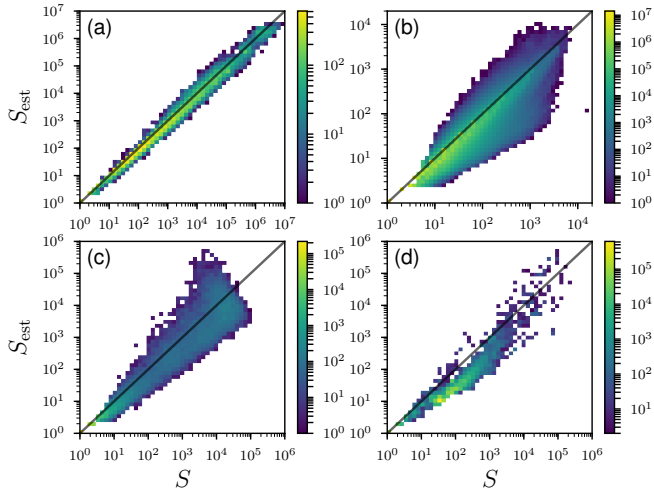


Fig. 2: Log-log-log histograms of the estimated abundance ( $S_{\text{est}}$  calculated as in (1)), versus actual abundance ( $S$ ) of the connected components of different GP maps: (a) four-letter RNA of length  $L = 16$ , (b) two-letter GC-RNA of length  $L = 30$ , (c) compact HP model  $5 \times 6$  with  $U(HH) = -1$ , and (d)  $t_{\text{OY}}\text{LIFE}$  for two genes.

but exhaustively folding longer sequences quickly becomes computationally unfeasible. Since NCs behave, to all purposes, as independent NNs, we treat them as independent phenotypes, regardless of whether or not they fold into the same secondary structure. Then, we count how many sequences each NC contains (its abundance,  $S$ ) and calculate its site versatilities  $v_i$  according to the definition (2). The product of them all yields the estimated abundance (1). Fig. 2(a) shows a histogram comparing actual and estimated abundances for all the NCs, showing a remarkable agreement. The distinction between NCs and phenotypes becomes less relevant as the length of genotypes grows, as discussed later (see also Appendix B).

A variant of this model is made of RNA sequences containing only two complementary bases, for example G and C (GC-RNA). A two letter alphabet allows us to study sequences almost twice as long with a similar computational effort [10]. We have repeated the previous analysis for GC-RNA sequences of length  $L = 30$ , and plotted the result in Fig. 2(b). Fragmentation is more frequent in this model, and NCs are generally smaller. This is why their number is so high and why they are so dispersed in Fig. 2(b). Also, the largest NCs are three orders of magnitude smaller than those of four-letter RNA sequences. For this model, the versatility of paired sites is strictly 1 because any mutation in such a pair will break the link. Unpaired sites do not have much more freedom either, because a mutation can often create a new link and change the folding. In spite of these constraints, Fig. 2(b) shows a clear correlation between  $S$  and  $S_{\text{est}}$ , with the overwhelming majority of NCs near the diagonal.

The third GP map that we have analysed is the HP

model for lattice proteins [23], where a protein is represented by a self-avoiding chain of hydrophobic (H) or polar (P) beads on a lattice. The energy of a given configuration is calculated from a contact potential,

$$E = \sum_{i < j} U(\sigma_i, \sigma_j) C_{ij} \quad (3)$$

where  $\sigma_i \in \{H, P\}$ ,  $C_{ij} = 1$  when  $i$  and  $j$  are neighbours on the lattice (with  $|i - j| \neq 1$ ) and  $C_{ij} = 0$  otherwise, and  $U(\sigma_i, \sigma_j)$  specifies the interaction strength. Several different specific realisations of the model can be found in the literature (see below). For two-dimensional square lattices, compact and non-compact versions of the model have been studied. In compact HP, sequences of length  $L = l_1 \times l_2$  are forced to fold into rectangular structures, while non-compact HP considers all self-avoiding walks in the lattice. In Fig. 2(c) we show the case example of compact HP  $5 \times 6$  with a single nonzero energy parameter,  $U(H, H) = -1$  where phenotype is defined as the non-degenerated, minimum energy conformation (see Appendix A).

Finally, we have also analysed  $t_{\text{OY}}\text{LIFE}$ , a multilevel model of a simplified cellular biology [24, 25] in which binary sequences are first mapped to HP-like proteins that interact between themselves, with the genome, and with metabolites. The phenotype is defined by the set of metabolites that a given sequence is able to catabolise. Consequently,  $t_{\text{OY}}\text{LIFE}$  has a lower genotype level, which translates into proteins (second level), whose interactions add a third, regulatory level. This regulation is altered as a result, giving rise to the phenotypic expression at this highest level. Even though the connection between genotype sites and structural elements in this model is far from clear, versatilities can be computed nonetheless. The estimations of phenotype abundances arising from their values, for the case of two genes (length  $L = 40$ ), are compared with actual abundances in Fig. 2(d). We can observe a slight but systematic underestimation of abundances. In spite of that, the correlation between  $S$  and  $S_{\text{est}}$  is strong, and the cloud of points runs parallel to the diagonal. The slight underestimation of versatility, however, does not affect the argument leading to the log-normal abundance distribution —only the mean and the variance will be affected.

The prediction of phenotype abundance has been a matter of study, among others due to its relevance for protein designability [26], for molecular robustness and evolvability [27], or in the neutralist-selectionist controversy [8]. Attempts at estimating phenotype abundance have been made using compositional entropy [23, 26]. However, the comparison with the predictions obtained through site versatility reveals that versatility has a superior performance (see Appendix C and Fig. S1).

**Distribution of abundance of RNA NCs.** — Figure 3(a) shows the distribution  $p(\ln S)$  of the abundance

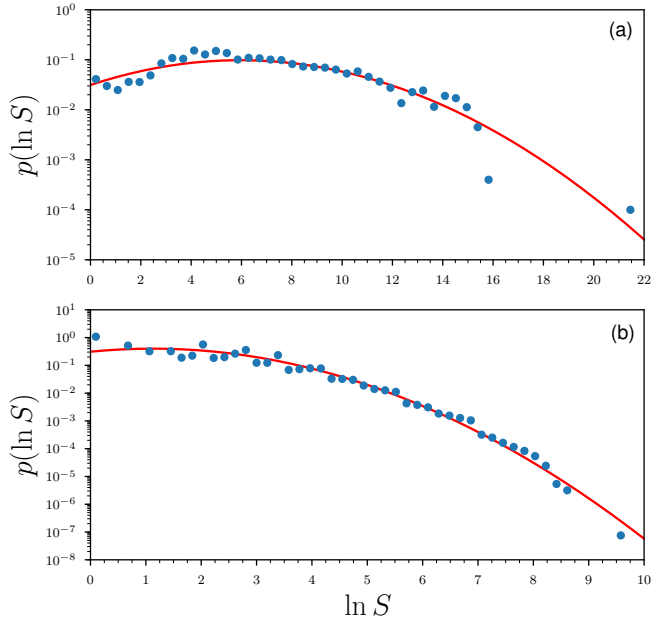


Fig. 3: Log-abundance distributions  $p(\ln S)$  for the the NCs of (a) four-letter RNA sequences of length  $L = 16$  and (b) GC-RNA sequences of length  $L = 30$ . Dots are the actual values; lines are Gaussian fits to the data.

of RNA sequences of length  $L = 16$  in NCs, along with a least-squares fit of the function  $\exp[a(\ln S)^2 + b \ln S + c]$ , the expected asymptotic distribution according to Eq. (1). The length of the sequences is too short to exhibit a perfect Gaussian shape yet: the curve is truncated on the left-hand side and there are deviations for small and large NCs abundances.

Though the abundance distribution of NCs for GC-RNA sequences is a decreasing function with a fat tail (Fig. 3(b)), the right tail of a log-normal provides a good fit that captures the slight concavity of the curve. Regardless of the alphabet size, the log-normal distribution is theoretically supported by Eq. (1).

The theory developed up to now strictly applies to NCs of phenotypes. However, it was originally inspired by studies reporting a log-normal distribution of *phenotype* abundances [8]. Also, data corresponding to GC-RNA phenotypes compatible with a power-law distribution [16] can be fit at least equally well by a truncated log-normal such as that in Fig. 3(b). In the next section we will introduce an effective model that will provide some insights into the specific shapes of these distributions and clarify how the theory asymptotically applies to phenotypes.

**Effective two-versatility model for RNA.** –

Consider long RNA sequences —irrespective of their composition— folded into secondary structures. It has been shown that paired and unpaired sites admit on average a different amount of mutations in a given NC, that is, they differ in neutrality. Asymptotically, the overall neutrality of a phenotype can be well described by two

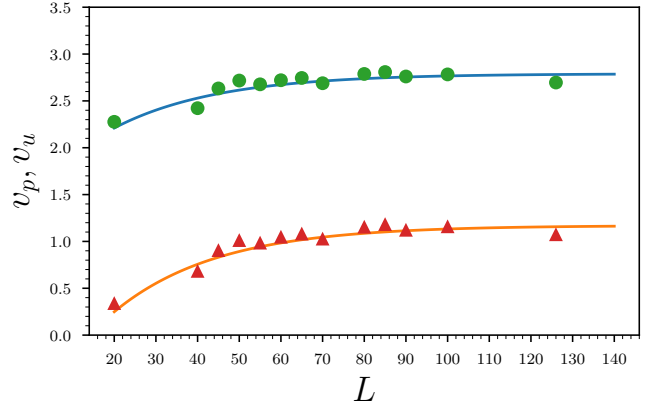


Fig. 4: Average versatilities of unpaired ( $v_u$ ) and paired ( $v_p$ ) sites obtained by fitting a two-versatilities model to the sampled abundance distributions of Ref. [8] for RNA sequences of different lengths. Lines are fits to data of the form  $v_i = v_i^\infty - b_i e^{-c_i L}$ , from which the asymptotic values of the two versatilities  $v_i^\infty$  are extrapolated.

values, each corresponding to one of the structural elements [28, 29]. In this vein, we consider now a simplified model with two versatility values: one for paired ( $v_p$ ) and one for unpaired ( $v_u$ ) sites (with  $1 \leq v_p < v_u \leq k$  for an alphabet of  $k$  letters). As neutrality, site versatility depends in principle on many factors other than whether the corresponding base forms a bond. Nevertheless, we do observe that, on average, versatilities associated to paired sites are significantly smaller than those associated to unpaired ones. Interestingly, previous works have identified a clear correlation between RNA secondary structure elements (stems and loops) and nucleotide composition [30,31], giving indirect support to our approximation.

The two-versatility model was introduced [20] to argue for a log-normal distribution of the abundance of RNA sequences in NNs. More precisely, the number of RNA secondary structures with a given number  $\ell$  of paired sites can be shown to be (in the limit  $L \rightarrow \infty$ ) proportional to a Gaussian function of  $\ell$  with mean  $\mu L - \mu_0$  and standard deviation  $\sigma L^{1/2} - \sigma_0 L^{-1/2} + O(L^{-3/2})$  ( $\mu = 0.28647$ ,  $\mu_0 = 1.36502$ ,  $\sigma = 0.25510$ ,  $\sigma_0 = 0.00713$ ). In virtue of (1) and the fact that, within the two-versatility model,  $S = v_p^\ell v_u^{L-\ell}$ —hence  $\ell \propto \log S$ —this immediately leads to a log-normal distribution of  $S$  with mean and standard deviation

$$\begin{aligned} \mu_L &= L(\ln v_u - \mu) + \mu_0 + O(L^{-1}), \\ \sigma_L &= 2 \ln(v_u/v_p) \left( \sigma L^{1/2} - \sigma_0 L^{-1/2} \right) + O(L^{-3/2}). \end{aligned} \quad (4)$$

In order to test this two-versatility model we will use the data of Ref. [8] —a collection of estimates of the abundance distribution of RNA secondary structures obtained by sampling random sequences of lengths in the range  $L = 20$ –126. The resulting distributions are proportional to  $S p(\ln S)$  but, if  $p(\ln S)$  is a normal distribu-

tion with mean  $\mu_L$  and standard deviation  $\sigma_L$ , then so is  $Sp(\ln S)$ , with the same standard deviation but a shifted mean  $\mu_L + \sigma_L^2$ . Fitting Gaussian functions to these data yields  $\mu_L$  and  $\sigma_L$ . Then, through Eqs. (4), (5) we can infer the corresponding versatilities  $v_p, v_u$ —which appear in Fig. 4. This plot suggests that these versatilities have well defined asymptotic values for  $L \rightarrow \infty$ , namely  $v_p = 1.17 \pm 0.08$ ,  $v_u = 2.79 \pm 0.08$ . For comparison, the average versatilities obtained from our data for  $L = 16$  are  $v_p^{\text{av}} = 1.11$ ,  $v_u^{\text{av}} = 2.37$ .

A caveat is in order here. The results of [8] correspond to the abundance of phenotypes, no matter how many NCs they have, whereas, strictly speaking, the two-versatility model can only be applied to the latter. The surprising agreement of the extrapolated versatilities with those directly obtained from the data for  $L = 16$  suggests that for  $L$  large, either phenotypes are broken into few NCs, or one of these components is much larger than the others and dominates the abundance of the phenotype. The existence of genetic correlations in NCs seems to cause both effects [6]. Even for short RNA and HP sequences, the largest connected component of a phenotype grows linearly with the abundance of the phenotype, while the number of components either diminishes with phenotype abundance [10] or remains mostly independent [32]. Therefore, the largest NC becomes more dominant the larger the phenotype, so that the latter is well approximated by a single component. In consequence, the distribution of phenotype abundances is asymptotically equivalent to the distribution of NCs abundances.

The improvement of the fit upon increasing length can be indirectly inferred from the data of Ref. [8]. The fits of Gaussian functions to these data are more accurate than the one of Fig. 3(a) (see Appendix D and Fig. S2), and show that the log-normal behaviour of  $p(S)$  is what should be expected for long sequences.

We can apply the two-versatility model to our results with GC-RNA. The effective versatilities are  $v_p = 0.75$  and  $v_u = 1.32$  (from the data we obtain the exact value  $v_p = 1$  and the average  $v_u^{\text{av}} = 1.43$ ). As in the case of four-letter RNA (c.f. Fig. 4), the values of  $v_p$  for short lengths are unphysical ( $v_p < 1$ ). This notwithstanding, effective versatilities are not too far from the average ones, providing an indirect support to the fact that the log-normal distribution for this model has a mean close to 1—explaining why only the right branch is observed.

**Phenotype definition, alphabet size, and navigability of genotype spaces.**— Figure 2 suggests that the goodness of the phenotype abundance estimation (1) might depend on the specific GP map. While it works amazingly well for four letter RNA, it is not that good for compact HP or  $\tau_{\text{OY}}\text{LIFE}$ , which have similarly large NCs. Indeed, high accuracy in that prediction implicitly relies (i) on the existence of a clear-cut quantitative relationship between sequence sites and structural elements—which is mediated by a consistent definition of phenotype, and (ii)

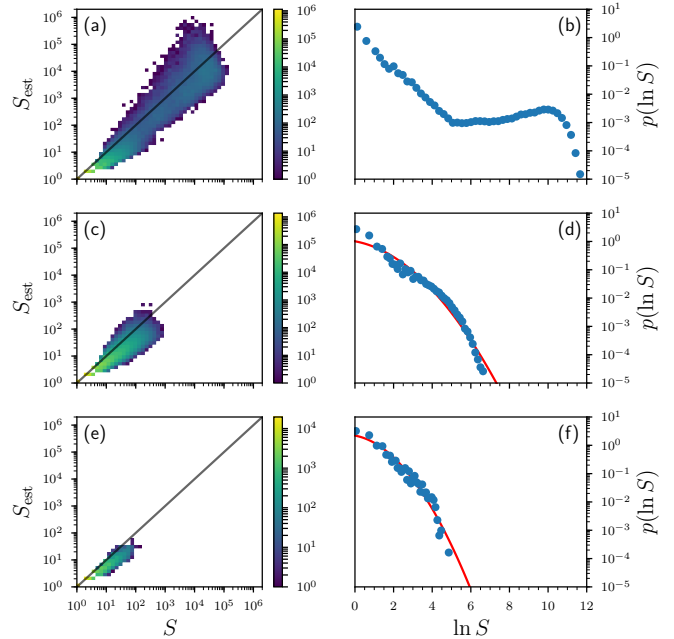


Fig. 5: (a, c, e)- Log-log-log histograms of the estimated abundance  $S_{\text{est}}$  versus actual abundance  $S$  of the NCs of different HP versions. (b, d, f) NCs abundance distributions. (a, b) Compact HP  $5 \times 6$  with  $U(H, H) = -2.3$  and  $U(H, P) = U(P, H) = -1$ , (c, d) non-compact HP30 with  $U(H, H) = -1$ , and (e, f) non-compact HP20  $\mathcal{S}$  (based on minimal contact maps) with  $U(H, H) = -1$ .

on the presence of a giant NC in phenotypes. The latter seems essential for the abundance of phenotypes to follow a *bona fide* log-normal distribution. Though the relationship between sequence and structure is unequivocal for RNA, it depends on the definition of phenotype in various versions of the HP model (see Appendix A), becomes unavoidably cryptic for  $\tau_{\text{OY}}\text{LIFE}$ , and might be hard to define in GP maps lacking an easy representation of genotypes as sequences [35]. On the other hand, a comparison of the distribution of abundances in two- and four-letter RNA indicates that the larger the alphabet the larger the components of phenotypes and the better defined the log-normal distributions. These observations are in full agreement with results for the HP model, as shown in the following.

Figure 5 illustrates the performance of versatility and abundance distributions for three additional definitions of phenotype in HP models: compact HP30 with two parameters for energy (Fig. 5 (a) and (b)), non-compact HP30 ((c) and (d)) and non-compact HP20 with phenotypes defined through *minimal* contact maps ((e) and (f)) that is, the set  $\mathcal{S}_{ij}$  formed by those pairs with a nonzero contribution to the folding energy,  $\mathcal{S}_{ij} = \{i, j \mid U(\sigma_i, \sigma_j)C_{ij} < 0\}$ .

Initially, the HP model was implemented in its compact version for computational tractability: notice that the number of different two-dimensional conformations in compact HP30 is  $10^8$ -fold smaller than in non-compact

Table 1: Data corresponding to the exhaustive enumeration of phenotypes in multiple GP maps. The first column lists the maps studied and some of its quantitative properties: total number of phenotypes, number of non-empty (NE) phenotypes (this quantity resulting from folds with non-negative energy and the large number of degenerated genotypes that are discarded, see Appendix A), number of sequences assigned to a unique phenotype (UaS), average abundance of phenotypes  $S_{av}$ , total number of neutral components (NCs), and fraction of non-functional sequences ( $f_\emptyset$ ). Non-compact HP20 (n-c HP20) is included to compare with n-c HP20 with minimal contact maps (n-c HP20  $\mathcal{S}$ ) as phenotypes (a distribution of phenotype abundances for n-c HP20 can be found in [33]). <sup>1</sup>Data obtained with two energy parameters,  $U(H, H) = -2.3$  and  $U(H, P) = U(P, H) = -1$ . <sup>2</sup>Data from [34].

Model	Phenotypes	NE phenotypes	UaS	$S_{av}$	NCs	$f_\emptyset$
RNA30 GC	240,944,076	432,221	1,073,725,603	2,484.2	68,389,814	0.0000151
RNA16 ACGU	5,223	648	1,712,323,320	2,642,474	23,092	0.601
compact HP30	13,498	13,498	187,212,435	13,869.6	362,221	0.826
compact HP30 <sup>1</sup>	13,498	13,498	258,434,457	19,146.1	1,986,907	0.759
n-c HP30 <sup>2</sup>	784,924,528,667	2,333,498	22,466,621	9.63	3,732,449	0.979
n-c HP20	41,889,578	5,310	24,900	4.69	6,586	0.976
n-c HP20 $\mathcal{S}$	910,971	54,818	292,732	5.34	62,379	0.721
$\text{toyLIFE}$	$2^{214} \simeq 2.63 \times 10^{64}$	775	134,400,450	173,419.9	1,523,544	0.9999

HP30 (Table 1). Compact HP versions actually impose unrealistic spatial constraints: two residues  $i$  and  $j$  can be forced to be in contact without having an associated interaction energy, that is  $C_{ij} = 1$ , but  $U(\sigma_i, \sigma_j) = 0$ . Spatial restrictions may therefore assign to a unique phenotype (or NC thereof) sequences whose affiliation easily changes under more natural phenotype definitions [36]. This has an immediate effect on abundance distributions, as Fig. 5(b) shows: besides a decrease at small NC sizes, the distribution develops a bump at high abundances. The non-compact versions of HP are difficult to explore exhaustively due to the astronomically large number of possible phenotypes [34]. Still, phenotypes are free from spatial constraints and, as a result, abundance distributions can be fit with a log-normal function (Fig. 5(d), (f)). These distributions are qualitatively similar to that obtained for GC-RNA, though NCs are significantly larger in the latter. Smaller NCs could be expected if, instead of the Vienna Package to fold RNA sequences, a model with few energy parameters (such as, e.g., Nussinov algorithm for loop matching [37]) is used.

In either compact or non-compact realisations, folding is calculated by using one [34] or two [23] nonzero energy parameters, examples being  $U(H, H) = -1$ , as in Fig. 2(c) or  $U(H, H) = -2.3$ , and  $U(H, P) = -1$ , e.g., as in Fig. 5(a)). Genotypes in these HP models can typically be mapped to more than one phenotype. Traditionally, these degenerated genotypes are discarded, since they have been interpreted as the analogues of intrinsically disordered proteins, and therefore devoid of function. This convention results in one of the most concerning features of classical HP models [38], where an astonishingly large fraction of sequences are systematically not assigned to phenotypes, yielding empty phenotypes and many small and highly fragmented ones (see Table 1 for representative examples). It is important to remark that a high

fraction of non-functional sequences does not necessarily imply that phenotypes are small and isolated, since other models —where the small fraction of functional sequences is not due to degeneration— do have large and easily navigable phenotypes [24, 39, 40].

Adding more energy parameters serves to disambiguate the assignation of genotypes to phenotypes, though the increase in the fraction of sequences assigned to phenotypes is however minor (compare the two compact HP30 versions in Table 1). Phenotypes defined through contact maps are closer analogues of RNA secondary structure (as in our example with non-compact HP20): contact maps appear as a more natural definition of phenotype that furthermore reduces about 40-fold the number of different phenotypes and notably decreases sequence degeneration (Table 1). Also, degeneration diminishes significantly when the size of the alphabet grows. In a systematic study with sequences of length  $L = 25$ , degeneration is halved when going from two- to four-letter alphabets, and it reaches a few percent for 20-letter representations [41]. Concomitantly, phenotypes become larger and more connected.

The fact that most phenotypes are small, weakly connected and even difficult to navigate in classical HP models [34] raises doubts on their relevance for evolutionary dynamics, speaking in favour of more complex but also more realistic scenarios [38], and certainly supporting non-compact versions of lattice protein models [36]. In agreement with the above, the definition of phenotype critically affects the distribution of abundances, which changes from decreasing functions for two-letter alphabets (as in Fig. 5) to functions with a maximum and a fat tail for 20-letter, compact versions [38, 42]. Independent studies suggest that minimal alphabets are not optimal in an evolutionary sense [43], further supporting the limited applicability of two-letter models, especially to draw conclusions on evolutionary dynamics. Unfortunately, an exhaustive study

of non-compact lattice protein models with more than two letters is, as of today, computationally unfeasible.

**Conclusions.** – The vastness of genotype spaces prevents a complete characterisation based on computational approaches. A look at Table 1 suffices to illustrate the astronomically large numbers involved in calculations with sequences of length well below that typically found in biochemical processes. The data generated to analyse the different models in this contribution reaches 0.5TB and, as their diversity shows, would be of limited use in the absence of an accompanying theory. Therefore, an understanding of the structure of realistic GP maps demands further theoretical developments that can be extrapolated to arbitrarily long sequences. We have shown that the definition of useful quantities such as versatility allows for reliable estimations of the abundance of phenotypes and for the derivation of the expected distribution. Knowledge of the asymptotic values  $v_p$  and  $v_u$  yields that distribution in RNA of any length, as well as an estimation of the number of genotypes folding into an arbitrary (typical) structure. Similar derivations should be possible for other GP maps endowed with consistent definitions of phenotype.

\*\*\*

K Dingle, E Ferrada, Ch Holzgräfe, A Irbäck and A Louis are gratefully thanked for sharing their data with us. We acknowledge financial support by the Spanish Ministerio de Economía y Competitividad and FEDER funds of the EU through grants VARIANCE (FIS2015-64349-P; PC, JAC) and ViralESS (FIS2014-57686-P; JAGM, SM).

## REFERENCES

- [1] COWPERTHWAIT M. C. and MEYERS L. A., *Annual Review of Ecology, Evolution, and Systematics*, **38** (2007) 203.
- [2] AGUIRRE J., CATALÁN P., CUESTA J. A. and MANRUBIA S., *ArXiv e-prints*, (2018) .
- [3] SCHUSTER P., FONTANA W., STADLER P. F. and HOFACKER I. L., *Proc. Roy. Soc. London B*, **255** (1994) 279.
- [4] BORNBERG-BAUER E., *Biophys. J.*, **73** (1997) 2393.
- [5] WAGNER A., *The origins of evolutionary innovations* (Oxford University Press) 2011.
- [6] AHNERT S. E., *J. R. Soc. Interface*, **14** (2017) 20170275.
- [7] SCHAPER S. and LOUIS A. A., *PLoS ONE*, **9** (2014) e86635.
- [8] DINGLE K., SCHAPER S. and LOUIS A. A., *J. Roy. Soc. Interface*, **5** (2015) 20150053.
- [9] CATALÁN P., ARIAS C. F., CUESTA J. A. and MANRUBIA S., *Biol. Direct*, **12** (2017) 7.
- [10] GRÜNER W., GIEGERICH R., STROTHMANN D., REIDYS C., WEBER J., HOFACKER I. L., STADLER P. F. and SCHUSTER P., *Monatshefte f. Chemie*, **127** (1996) 375.
- [11] FONTANA W. and SCHUSTER P., *J. Theor. Biol.*, **194** (1998) 491.
- [12] SCHUSTER P. and STADLER P. F., *Computers Chem.*, **18** (1994) 295.
- [13] GRÜNER W., GIEGERICH R., STROTHMANN D., REIDYS C., WEBER J., HOFACKER I. L., STADLER P. F. and SCHUSTER P., *Monatshefte f. Chemie*, **127** (1996) 355.
- [14] SCHUSTER P., *Rep. Prog. Phys.*, **69** (2006) 1419.
- [15] STICH M., BRIONES C. and MANRUBIA S. C., *J. Theor. Biol.*, **252** (2008) 750.
- [16] FERRADA E. and WAGNER A., *Biophys. J.*, **102** (2012) 1916.
- [17] COWPERTHWAIT M. C., ECONOMO E. P., HARCOTBE W. R., MILLER E. L. and MEYERS L. A., *PLoS Comput. Biol.*, **4** (2008) e1000110.
- [18] AGUIRRE J., BULDÚ J. M., STICH M. and MANRUBIA S. C., *PLoS ONE*, **6** (2011) e26324.
- [19] GREENBURY S. and AHNERT S., *J. R. Soc. Interface*, **12** (2015) 20150724.
- [20] MANRUBIA S. and CUESTA J. A., *J. R. Soc. Interface*, **14** (2017) 20160976.
- [21] CUESTA J. A. and MANRUBIA S., *J. Theor. Biol.*, **419** (2017) 375.
- [22] LORENZ R., BERNHART S. H., HÖNER ZU SIEDERDISSEN C., TAHER H., FLAMM C., STADLER P. F. and HOFACKER I. L., *Algorithms for Molecular Biology*, **6** (2011) 26.
- [23] LI H., HELLING R., TANG C. and WINGREEN N., *Science*, **273** (1996) 666.
- [24] ARIAS C. F., CATALÁN P., MANRUBIA S. and CUESTA J. A., *Sci. Rep.*, **4** (2014) 7549.
- [25] CATALÁN P., WAGNER A., MANRUBIA S. and CUESTA J. A., *J. Roy. Soc. Interface*, **15** (2018) 20170516.
- [26] LARSON S. M., ENGLAND J. L., DESJARLAIS J. R. and PANDE V. S., *Protein Sci.*, **11** (2002) 2804.
- [27] JÖRG T., MARTIN O. C. and WAGNER A., *BMC Bioinformatics*, **9** (2008) 464.
- [28] HUYNEN M. A., *J. Mol. Evol.*, **43** (1996) 165.
- [29] REIDYS C. M., FORST C. V. and STADLER P. F., *Bull. Math. Biol.*, **63** (2001) 57.
- [30] SCHULTES E. A., HRABER P. T. and LABEAN T. H., *RNA*, **3** (1997) 792.
- [31] SMIT S., YARUS M. and KNIGHT R., *Bioinformatics*, **12** (2006) 1.
- [32] GREENBURY S. F., SCHAPER S., AHNERT S. E. and LOUIS A. A., *PLoS Comput. Biol.*, **12** (2016) e1004773.
- [33] SHAHREZAEI V., HAMEDANI N. and EJTEHADI M. R., *Phys. Rev. E*, **60** (1999) 4629.
- [34] HOLZGRÄFE C., IRBÄCK A. and TROEIN C., *J. Chem. Phys.*, **135** (2011) 195101.
- [35] IBÁÑEZ-MARCELO E. and ALARCÓN T., *J. Theor. Biol.*, **356** (2014) 144.
- [36] IRBÄCK A. and TROEIN C., *J. Biol. Phys.*, **28** (2002) 1.
- [37] NUSSINOV R., PIECZENIK G., GRIGGS J. R. and KLEITMAN D. J., *SIAM J. Appl. Math.*, **35** (1978) 68.
- [38] BUCHLER N. E. G. and GOLDSTEIN R. A., *Proteins*, **34** (1999) 113.
- [39] CILIBERTI S., MARTIN O. C. and WAGNER A., *Proc. Natl. Acad. Sci. USA*, **104** (2007) 13595.
- [40] MATIAS RODRIGUES J. F. and WAGNER A., *PLoS Comp. Biol.*, **5** (2009) e1000613.
- [41] BUCHLER N. E. G. and GOLDSTEIN R. A., *J. Chem. Phys.*, **112** (2000) 2533.
- [42] LI H., TANG C. and WINGREEN N. S., *Proteins*, **49** (2002) 403.
- [43] GARDNER P. P., HOLLAND B. R., MOULTON V., HENDY

- M. and PENNY D., *Proc. R. Soc. Lond. B*, **270** (2003) 1177.
- [44] TURNER D. H. and MATHEWS D. H., *Nucleic Acids Res.*, **38** (2010) 280.
- [45] ZUKER M. and STIEGLER P., *Nucleic Acids Res.*, **9** (1981) 133.

**APPENDIX A: Phenotype definitions.** — There is no unique, unambiguous or optimal definition of phenotype. In general, it is an environment-dependent quantity that may take a variety of forms in computational models as those studied in this work. On the positive side, most statistical properties of the genotype-phenotype map are independent (or weakly dependent) on the precise definition.

*RNA.* The most used energy model for RNA secondary structure folding [44] is based on experimentally measured energy contributions of hydrogen bonds and stacking interactions between paired and adjacent nucleotides, energetically unfavourable unpaired regions, such as hairpin loops, bulges, internal loops and multiloops, and specific favourable contributions, such as GNRA tetraloops. The minimum free energy structure of a given RNA chain (genotype) can be thus determined by applying Zuker’s dynamic programming algorithm [45] with the given energy model.

RNA GP maps are constructed by assigning to each genotype its minimum free energy secondary structure as phenotype. In cases when the folding energy is negative, there might be still more than one secondary structure with the same (minimum) energy. In general, when a genotype can be assigned to more than one phenotype it is said to be *degenerated*. RNA folding algorithms, however, randomly select one of those minimum energy structures and assign the genotype to that phenotype. When the folding energy is non-negative, the corresponding phenotype is then the empty phenotype (the open structure with no base pairs) and the genotype is considered as *non-functional*.

*HP model.* HP models consider chains of hydrophobic and polar amino acids (genotypes) placed in a two or three dimensional lattice, which imposes spatial folding constraints. Depending on the size of that lattice the model can be *compact* or *non compact*. In compact models the lattice size is finite, and in the case considered in this work it equals the protein length. The size of the lattice forces proteins to fit into a given space applying the rationale that proteins preferentially fold into globular structures. This assumption drastically reduces the number of possible phenotypes. On the other hand, *non-compact* models consider an infinite lattice, where possible conformations are only limited by the protein backbone and the spaces occupied by other amino acids.

An often used definition of phenotype in HP models is the conformation or *path* in which it has the lowest free energy. Phenotype is therefore characterized by the path followed by the backbone of the sequence on the lattice

(after symmetries are eliminated), regardless the number or position of actual contacts between residues. This is the basic definition we use for HP compact and non-compact models in the main text if no variant is specified. In this context, it is usually assumed (at odds with RNA) that if a protein can fold into more than one conformation with the same minimum energy the phenotype is ambiguous and the genotype is *degenerated*. Classical approaches consider degenerated genotypes as *non-functional*, and therefore discard the corresponding genotypes, which are not included in further analyses. Given the small number of parameters involved in energy calculations, degeneration occurs very frequently, leading to a perhaps surprisingly high number of non-functional sequences in HP models (a quantity that includes folds with non-negative energy but also folds with negative energy if they are degenerated). As a result, most of the possible phenotypes are empty, just because compatible genotypes happen to yield more than one minimum free energy conformation. Non-compact HP models are especially affected by degenerated genotypes due to the conformational freedom intrinsic to non-interacting parts of the genotype.

Degeneration is a somehow artefactual property that can be reduced under more realistic definitions of phenotype, for example by using a different energy model. The simplest model (HH) considers only interactions between hydrophobic amino acids, assigning an energy of -1 to each H-H interaction. An alternative energy model used in this work also assigns an energy to hydrophobic-polar interactions ( $H-H = -2.3$  and  $H-P = -1$ ). Another possibility is to use *minimal contact maps* to define phenotypes. The minimal contact map of a sequence minimizes the free energy and also the number of non energetically favourable contacts (energy  $\leq 0$ ). This definition can account for the contribution of non favourable interactions (which can be weak compared with hydrophobic interactions, but should not be ignored) and discards conformational changes due to non-interacting parts of the genotype. Note that this definition is similar to RNA secondary structure models defined by sets of paired and unpaired regions.

**Appendix B: Computing versatilities using connected components instead of the whole neutral network.** — In the main text, we consider the different connected components of a phenotype to be different phenotypes in order to estimate their abundances. The reason for this is that if we compute the versatilities lumping all connected components together, the abundance of the phenotype is typically greatly overestimated, unless one of the connected components dominates the neutral network—in which case lumping or not makes little difference.

To understand why this is so we can use a very simple example. Suppose a phenotype that is codified by the following sequences:

000000	010000	100000	110000
001111	011111	101111	111111

Clearly, each row belongs to a different connected component, because all genotypes in the upper row end in 0000, and all the genotypes in the lower row end in 1111 (for a GP map such as toyLIFE, this situation is not uncommon). Calculating site versatilities with our formula (c.f. Eq. (2) in main text) for each separate connected component we obtain

$$v_1 = v_2 = 2, \quad v_3 = v_4 = v_5 = v_6 = 1. \quad (6)$$

Estimating the size of these components with Eq. (1) (main text) then leads to the correct result  $S = 4$  for both of them. However, if we lump together all genotypes into a single phenotype Eq. (2) (main text) estimates site versatilities as  $v_i = 2$  for all sites, and so the size estimate obtained from Eq. (1) will be  $2^6 = 64$ , 8 times larger than the actual abundance.

From this example one can also understand why, if one of the connected components is much larger than the rest, the distortion of lumping all components together will have a small effect on our estimate of phenotype abundance.

**APPENDIX C: Estimating phenotype abundance using compositional entropy.** – In the main text, we present one way to estimate the abundance of a phenotype by defining the versatility of a site  $i$  as

$$v_i = \frac{1}{M_i} \sum_{\alpha=1}^k m_{\alpha,i}, \quad M_i \equiv \max\{m_{1,i}, \dots, m_{k,i}\}, \quad (7)$$

where  $m_{\alpha,i}$  is the number of genotypes of the phenotype in which the letter  $\alpha$  appears at site  $i$ , and  $k$  is the size of the alphabet. The estimated abundance of a phenotype  $S_{\text{est}}$  would then be given by

$$S_{\text{est}} = \prod_{i=1}^L v_i. \quad (8)$$

Previous work [23,26] had proposed a different formula for the estimation of phenotype abundance using compositional entropy:

$$p_i = - \sum_{\alpha=1}^k \frac{m_{\alpha,i}}{M_S} \ln \left( \frac{m_{\alpha,i}}{M_S} \right), \quad M_S \equiv \sum_{\alpha=1}^k m_{\alpha,i}, \quad (9)$$

The abundance of the phenotype would then be computed as

$$S_{\text{est}} = \prod_{i=1}^L \exp(p_i). \quad (10)$$

In Figure S1 we test how well this formula predicts phenotype abundance, comparing actual abundances with estimates for the four models studied in the main text, namely (a) RNA sequences of length  $L = 16$ , (b) two-letter GC-RNA sequences of length  $L = 30$ , (c) compact HP proteins folding on a  $5 \times 6$  lattice ( $L = 30$ ), and (d) toyLIFE genotypes with two genes ( $L = 40$ ).

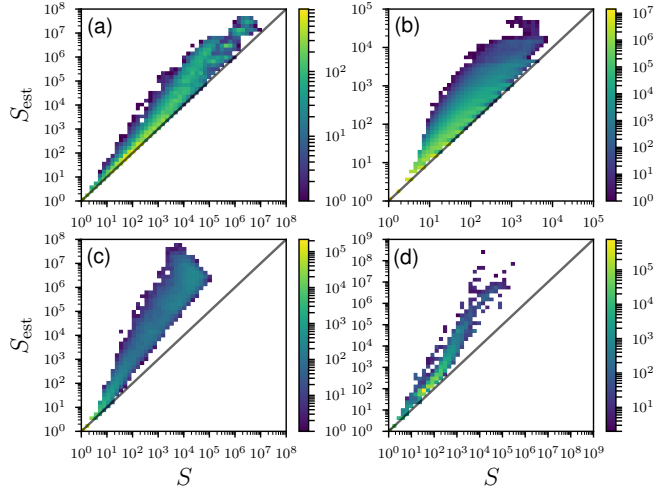


Fig. S1: Log-log-log histograms of the estimated abundance ( $S_{\text{est}}$ ) calculated using compositional entropy (see main text), versus actual abundance ( $S$ ) of the connected components of different GP maps: (a) four-letter RNA of length  $L = 16$ , (b) two-letter GC-RNA of length  $L = 30$ , (c) compact HP model  $5 \times 6$  with  $U(HH) = -1$ , and (d) toyLIFE for two genes.

In all cases, compositional entropy overestimates phenotype abundance. Worse, the prediction seems to follow a power law  $S_{\text{est}} \propto S^\gamma$ , with  $\gamma > 1$  and depending on the model. This means that the most abundant phenotypes are overestimated the most. This is an undesirable property, as abundant phenotypes are the ones that do appear in nature [8].

We can try to correct this method by taking into account correlation between sites, estimating the logarithm of phenotype abundance by

$$\ln S_{\text{est}} = - \frac{1}{L-1} \sum_{\alpha,\beta=1}^k \sum_{i=1}^L \sum_{j>i} p_{ij}^{\alpha\beta} \ln p_{ij}^{\alpha\beta}, \quad (11)$$

where  $p_{ij}^{\alpha\beta}$  is the probability that the symbol  $\alpha$  appears at site  $i$  and symbol  $\beta$  appears at site  $j$ . If  $p_{ij}^{\alpha\beta} = p_i^\alpha p_j^\beta$ , that is, if there are no correlations, this formula reduces to (10). The results (not shown) are very similar to those in Fig. S1, implying that correlations are not the source of the mismatch between predicted and actual abundances. In summary, compositional entropy is not a good method to estimate phenotype abundance.

**APPENDIX D: Fitting log-normal functions to abundance distributions of RNA secondary structures.** – Ref. [8] presented a collection of estimates of the abundances of RNA secondary structures for sequences of length  $L = 20$  to  $L = 126$ , obtained by random sampling of RNA sequences. The resulting distributions (shown in Fig. S2 with Gaussian fits) are proportional to  $Sp(\ln S)$ , since the process of choosing a phenotype of abundance  $S$  (with probability proportional to  $S$ ) is

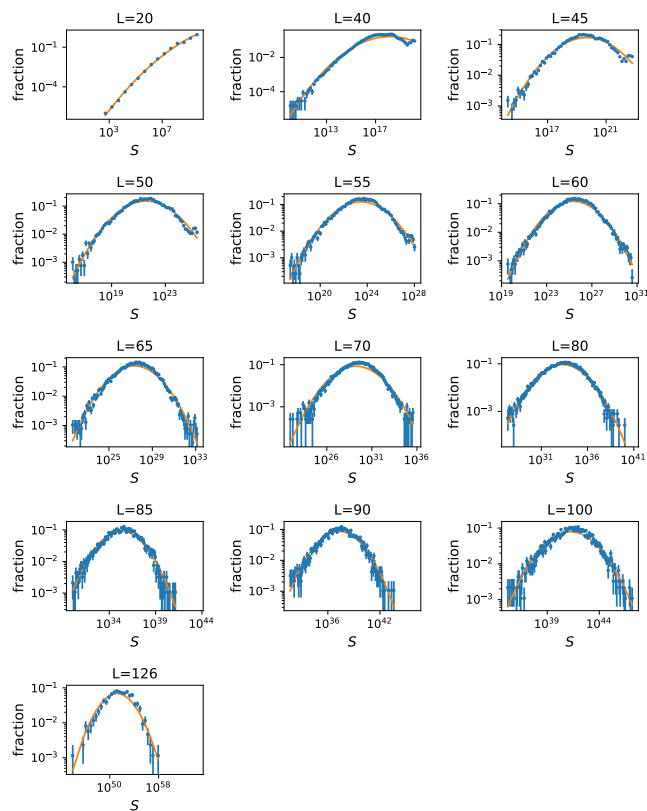


Fig. S2: Log-normal fits to the abundance distributions of RNA secondary structures from Ref. [8], for RNA sequences of lengths from  $L = 20$  to  $L = 126$ . The  $x$ -axes represent phenotype abundance  $S$  (in logarithmic scale), while the  $y$ -axes represent the fraction of phenotypes of abundance  $S$  when sampling at random among all possible genotypes. These fractions are proportional to  $Sp(\ln S)$ .

weighted by the number of phenotypes with that abundance, which is given by  $p(\ln S)$ . This distribution will follow a normal distribution if  $p(\ln S)$  does as well, but with a shifted mean (Fig. S2). This shift explains why the distribution of abundances of secondary structures for  $L = 20$  is increasing, contrasting with the rest of distributions we show in the main text.